

One-dimensional snow water and energy balance model for vegetated surfaces

Jiming Jin,² Xiaogang Gao,^{1*} Soroosh Sorooshian,¹ Zong-Liang Yang,¹ Roger Bales,¹ Robert E. Dickinson,¹ Shu-Fen Sun² and Guo-Xiong Wu²

¹*Department of Hydrology and Water Resources, University of Arizona, Tucson, AZ 85721, USA*

²*LASG, Institute of Atmospheric Physics, CAS, Beijing, China 100080*

Abstract:

We developed and evaluated a three-layer snow model for application in general circulation models. This one-dimensional snow model has many features of the detailed physically based model SNTHERM, yet is computationally much simpler. We have also extended the point model to vegetated areas using the parameterization concepts of the Biosphere-Atmosphere Transfer Scheme (BATS). Results of model applications for two types of vegetated fields — a short grassland in the French Alps and an old aspen forest in the southern study area of BOREAS — were presented. The results, on one hand, indicate the suitability of the model structure and parameter setting; on the other hand, the results explore the limitation of using ‘point’ field observations to evaluate an area model. Copyright © 1999 John Wiley & Sons, Ltd.

KEY WORDS land-surface scheme; snow model; surface heterogeneity; parameterization

NOMENCLATURE

C_D	= surface drag coefficient
C_l	= specific heat of water (4217.7) ($\text{J kg}^{-1} \text{K}^{-1}$)
c_p	= specific heat of air ($\text{J kg}^{-1} \text{K}^{-1}$)
C^p_R	= liquid water-holding capacity
C_v	= volumetric specific heat of snow ($\text{J m}^{-3} \text{K}^{-1}$)
d_s	= grid-average snow depth (m)
E	= rate of evaporation (upward is positive) ($\text{kg s}^{-1} \text{m}^{-2}$)
f_g	= wetness factor (1.0 at snow surface)
f_{ice}	= ice mass fraction
f_{snow}	= snow fractional coverage
f_{veg}	= vegetation fractional coverage (without snow)
H	= heat content for unit volume of snow (J m^{-3})
I_{sen}	= sensible heat flux (W m^{-2})
I_{prec}	= heat flux of precipitation (W m^{-2})
I_s^\downarrow	= downwelling solar radiation (W m^{-2})

* Correspondence to: X. Gao, Department of Hydrology and Water Resources, University of Arizona, Tucson, AZ 85721, USA. Email: jjm@hwr.arizona.edu or gao@hwr.arizona.edu

Contract grant sponsor: NASA/EOS Interdisciplinary Research Program.

Contract grant number: NAG53640 1 and NAGW-2062.

Contract grant sponsor: NOAA GCIP Program.

Contract grant number: NA46GP0247.

K	= snow thermal conductivity ($\text{W m}^{-1} \text{K}^{-1}$)
K_{soil}	= soil thermal conductivity ($\text{W m}^{-1} \text{K}^{-1}$)
L_{AI}	= leaf area index
L_{li}	= the heat of fusion (J kg^{-1})
L_{lv}	= latent heat of evaporation (J kg^{-1})
L_{net}	= net long-wave radiation (W m^{-2})
m_{ice}	= ice mass in a snow layer Δz (kg)
P_0	= effective rate of precipitation on land surface (downward is positive) ($\text{kg m}^{-2} \text{s}^{-1}$)
P_s	= snow load mass or overburden (kg m^{-2})
q_{af}	= specific humidity in the canopy
q_{air}	= air specific humidity above the canopy
q_{sn}	= air specific humidity at the snow surface
R_f	= liquid flow ($\text{kg m}^{-2} \text{s}^{-1}$)
R_{ough}	= surface roughness (m)
R_s	= net radiation at depth (W m^{-2})
R_s^n	= net surface solar radiation (W m^{-2})
t	= time (s)
T_{af}	= canopy air temperature (K)
T_{air}	= air temperature (K)
T_f	= leaf temperature (K)
T_p	= precipitation temperature (K)
T_{sn}	= snow surface temperature (K)
V_{af}	= $V_a C_D^{1/2}$, wind speed within the canopy (m s^{-1})
V_a	= wind speed at reference height (m s^{-1})
W_C	= $0.004 U_{af}$ (m s^{-1})
W_G	= $V_a C_D$ (m s^{-1})
z	= vertical coordinate (upward positive)
α	= snow surface albedo
γ_i	= $\rho_s f_{ice}$ = partial density of ice (kg m^{-3})
γ_l	= $\rho_s (1 - f_{ice})$ = partial density of liquid water (kg m^{-3})
ε_f	= thermal emissivity of leaf
ε_{air}	= thermal emissivity of air
σ	= Stefan-Boltzmann constant ($5.669 \times 10^{-8} \text{W m}^{-2} \text{K}^{-4}$)
η_0	= snow viscosity coefficient at $T = 273.15 \text{K}$ ($3.6 \times 10^6 \text{kg s m}^{-2}$)
θ_Z	= solar zenith angle (radians)
ρ_a	= density of air (kg m^{-3})
ρ_l	= density of liquid water (1000kg m^{-3})
ρ_s	= density of snow (kg m^{-3})
Δt	= time step (s)
Δz	= snow node thickness (m)

INTRODUCTION

Snow cover on land alters the energy and water interactions among the atmosphere, vegetation, and land, and provides significant water resources for many large-scale regions. Because of the importance of snow in global and regional climate and hydrology, a snow model is an essential component in coupled atmosphere and land-surface models, such as the General Circulation Models (GCMs). In the early versions of GCM snow models (such as BATS and SiB), snow temperatures were calculated using the modified force-restore method for a composite with a snow layer overlying soil (Dickinson, 1988). Diurnal variations were treated

by including a layer of approximately the diurnal penetration depth (about 0.1 m) in the snow-soil composite; over a season, penetration depth is on the order of a few meters. The corresponding heat flux to the bottom of the snow is neglected. Snowmelt is calculated through the surface energy balance. In addition, because heterogeneity across the landscape is important for both albedo and conductive and atmospheric flux transfers, the functions of soil, vegetation, and snow in a GCM grid square are parameterized.

Both the diurnal and seasonal time scales are important for climate modelling, and from the climate and hydrological viewpoint, the most crucial time for snow modelling is during the spring snowmelt period. Many studies for improvements have been conducted recently to involve a more detailed physical description of snow processes in GCMs (Verseghy, 1991; Loth *et al.*, 1993; Marshall *et al.*, 1994; Lynch-Stieglitz, 1994; Douville *et al.*, 1995; Pollard and Thompson, 1995; Bonan, 1996; Walland and Simmonds, 1996). These developments incorporated features found in 'point' snow property and process models (e.g., Anderson, 1976; Jordan, 1991). They are: (1) using coupled snow and soil heat transfer models instead of the force-restore approach for the snow-soil composite, (2) improving parameterization of snow properties, especially relating snow density to various compaction mechanisms, (3) describing the influence of the liquid phase on snow properties and processes, meanwhile using the concept of liquid water-holding capacity to simplify the simulation of water flow, and (4) using limited snow layers to reduce the model bias caused by the great variation in temperature and density along the snow depth.

We have developed a three-layer snow model for use in GCMs which is a simplification of the complex one-dimensional snow property and process model (SNTHERM89 Version 4.0) of Jordan (1991). The original 'point' model of SNTHERM assumes that the snow cover overlies a homogeneous surface, say, over a bare flat soil, and requires a large number of computations to describe the multi-phase physical processes in the snow pack. To represent snow cover on more realistic areas with a heterogeneous surface and to make the snow computation compatible to a large-scale coupled atmosphere and land-surface model, work is needed to extend and modify the SNTHERM model. First, three major simplifications were made in the structure of SNTHERM to reduce the computation. The new point model has been tested in a bare soil case against the field data. The results are in good agreement with the observations and with Jordan's model (Jin *et al.*, 1999). Then, this snow model coupled with a soil model (not described here) replaces the force-restore calculation in BATS (the vegetation model is the same). In the new land-surface scheme, we treat the heterogeneous surface by parameterizing the snow, soil, and vegetation patches into an areal mixture with fractional coverage for each surface type, which is taken from the concepts of the Biosphere-Atmosphere Transfer Scheme (BATS) (Dickinson *et al.*, 1993; Yang *et al.*, 1997). However, in BATS, vegetation and soil are modelled separately and then coupled, but as described above, snow and soil are treated as a composite except in calculating grid skin albedo and drag coefficient. In this paper, we introduce and test this grid-based snow model using the field data from France (grassland) and BOREAS (forest area) to evaluate the model performance in these two different land covers. We then assess whether any shortcomings in model performance are due to model limitations or to data limitations.

MODEL DEVELOPMENT

Our model differs from the physically detailed energy balance model, SNTHERM (Jordan, 1991), in three main aspects. First, our model does not consider the vapour phase; grain size determined through the vapour flow in SNTHERM was parameterized by the snow density. Second, the gravitational flow of liquid water in SNTHERM was replaced by the concept of 'liquid water-holding capacity' which was also parameterized by the snow density (Anderson, 1976; Loth *et al.*, 1993). Third, only three snow layers were used for the simulation. The layer division must vary following the movement of the snow surface. For a snow cover thicker than 40 cm, the top 20 cm of snow is divided into two layers with the top layer being 2 cm thick. For a snow thickness of 40 cm down to 6 cm, the top layer is still 2 cm, and the remaining part is divided equally into two layers; if the snow depth decreases from 6 cm, the number of snow layers reduces to 2 and then 1. Finally, a 5-mm thick snow cover is neglected and the water is added into soil (as ice or liquid water

depending on soil temperature). With these simplifications, the computation time steps in the algorithm can be fixed from 15 to 60 minutes.

Landscape heterogeneity of soil, vegetation, and snow cover must be represented in order to extend a point snow model to one representing a grid square. Here, we adopted the parameterization approach of BATS. Without snow, the soil surface of a grid square is partially covered with vegetation, which is described by the fractional foliage coverage (f_{veg}). As f_{veg} varies with the vegetation type and seasons, the same percentage of soil surface is treated as soil 'under the canopy', and the remaining portion of soil surface ($1 - f_{veg}$) is 'open to the atmosphere', called 'bare soil' (Figure 1). During a snow season, snow (partially) covers both the vegetation and bare soil. The fractional coverage of snow for these two grid portions needs to be estimated separately and then combined together. As shown in Figure 1, there are three snow cover components in a grid square:

- (1) fraction of snow on the bare soil portion and open to the atmosphere, which occupies $f_{snow}^{soil} \cdot (1 - f_{veg})$ percentage of the grid area,
- (2) fraction of snow on the vegetation portion and also open to the atmosphere, which occupies $f_{snow}^{veg} \cdot f_{veg}$ percentage of the grid area, and
- (3) fraction of snow in the vegetation portion but under the canopy, which occupies $f_{snow}^{soil} \cdot [(1 - f_{snow}^{veg}) \cdot f_{veg}]$ percentage of the grid area.

Notice that, the above fraction expressions are the products of two factors, in which f_{snow}^{soil} and f_{snow}^{veg} are estimated through equation (1) with $R_{ough} = 0.01$ m and $R_{ough} =$ vegetation roughness height (m), respectively (Dickinson *et al.*, 1993):

$$f_{snow} = \frac{d_s}{d_s + 10 \cdot R_{ough}} \quad (1)$$

where d_s is the average snow depth (m), and the second factors represent the grid portions which f_{snow}^{soil} and f_{snow}^{veg} are related to.

The combination of these three snow fractions, two in open areas and one under the canopy, constitutes the single snow cover of the grid square and will be described by the model. In the model, the snow cover is divided vertically into layers, but the snow state variables for each layer (e.g., temperature and water content) are parameterized to be horizontally 'effective' for the entire layer, and water and energy balance equations are used to solve these state variables for all snow layers. In order to model the effects of heterogeneous processes across the grid square, it is crucial to identify the fractions of snow surface in the open area and under the canopy. The fractions of bare soil, vegetation, and open-area snow cover (snow cover under the canopy is not included) are used as areal weights to calculate skin (grid-averaged surface) properties for the atmospheric model, such as albedo and drag coefficient. When calculating the energy, water and radiation fluxes on the snow surface, the different fractions of snow surface will deal with different environmental conditions (Figure 1 and Table III). Surface fluxes from snow surface in the open area are calculated through the interactions between the snow surface state variables (e.g., T_{sn} and q_{sn}) and the temperature (T_a), humidity (q_a), wind speed (V_a), and radiation of the low-level atmosphere, while surface fluxes from under the canopy snow cover are calculated through the interactions between the same snow state variables and the corresponding canopy-air variables (with subscript of 'af') calculated by the vegetation model of the land-surface scheme (Dickinson *et al.*, 1993).

In Figure 1, we try to illustrate a conceptually realistic representation of the fractional expressions of soil, vegetation and snow. This, however, is not the case within the model where all these components are uniformly blended according to their fractional coverage.

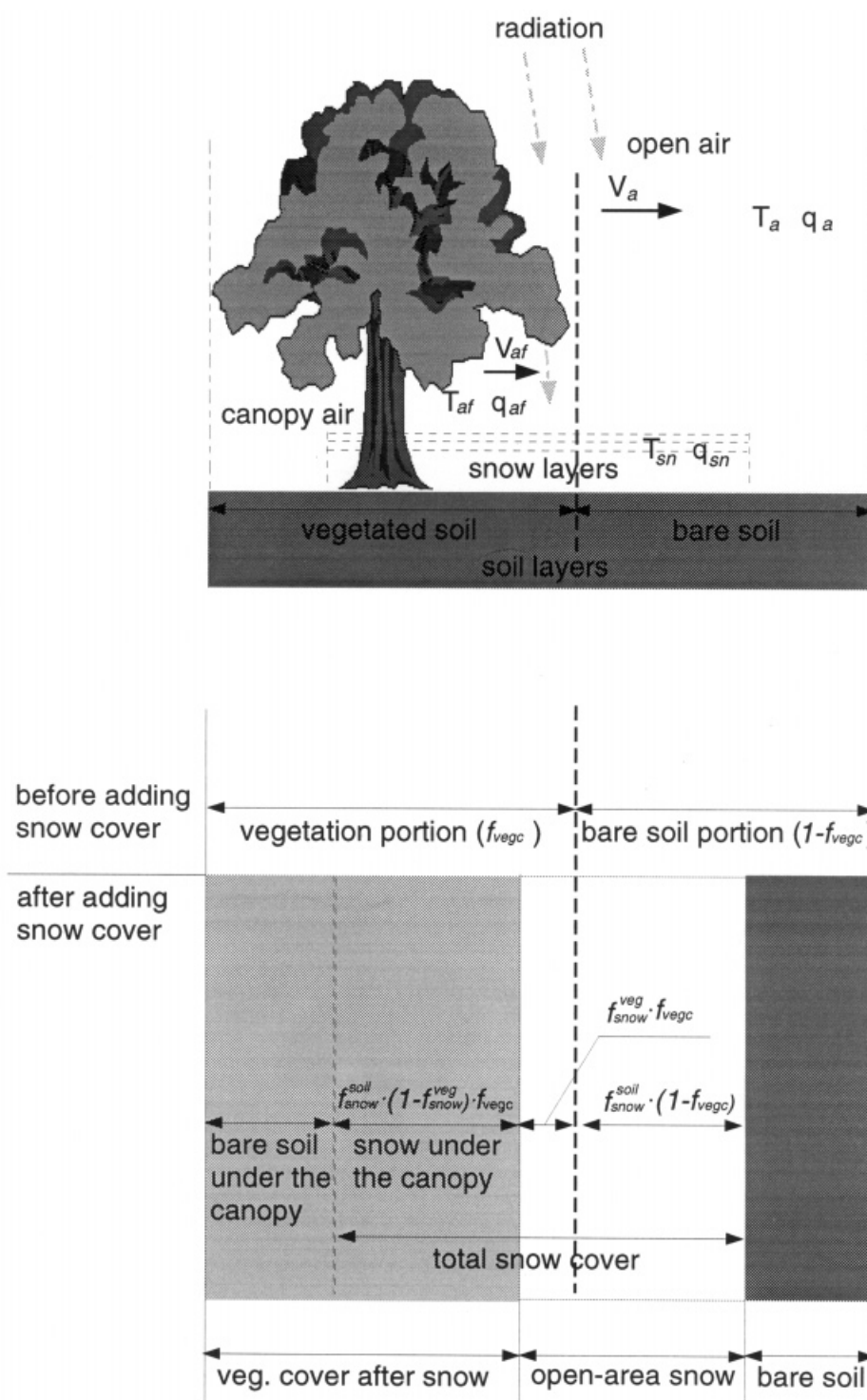


Figure 1. Concept illustration of modeling snow, vegetation, and soil and their fractional coverage in a grid square

Table I. Three snow compaction processes

	Metamorphism	Overburden	Melt
Snow compaction (Jordan, 1991)	$-2.8 \times 10^{-6} c_1 c_2 e^{-(273.15-T)/25}$	$-\frac{P_s}{\eta_0} e^{-C_3(273.15-T)} e^{-C_4 \rho_s}$	$-\frac{melt_rate}{\gamma_i \Delta z}$
$(\frac{1}{\Delta z} \frac{\partial \Delta z}{\partial t})$	$c_1 = c_2 = 1$ $c_1 = e^{-0.046(\gamma_i - 150)}, c_2 = 1$ $c_1 = 1, c_2 = 2$ $c_1 = e^{-0.06(\gamma_i - 150)}, c_2 = 2$	$(\gamma_l = 0, \gamma_i \leq 150 \text{ kg m}^{-3})$ $(\gamma_l = 0, \gamma_i > 150 \text{ kg m}^{-3})$ $(\gamma_l > 0, \gamma_i > 150 \text{ kg m}^{-3})$ $(\gamma_l > 0, \gamma_i > 150 \text{ kg m}^{-3})$	$\gamma_i < 250 \text{ kg m}^{-3}$ $\gamma_i \geq 250 \text{ kg m}^{-3}$
		η_0 $c_3 = 0.08 \text{ K}^{-1}$ $c_4 = 0.023 \text{ m}^3/\text{kg}^{-1}$	0

Three prognostic variables of snow density (ρ_s), heat content (H), and snow layer thickness (Δz) are solved through the mass and energy equation and the snow compaction model (adopted from the revised SN THERM codes) (Table I).

Mass conservation (continuity) equation

The snow density (ρ_s including both liquid and ice mass described by the ice mass fraction of snow f_{ice}) changes because of snow compaction and flow of liquid water, R_f :

$$\frac{\partial \rho_s}{\partial t} + \frac{\rho_s}{\Delta z} \frac{\partial \Delta z}{\partial t} = \frac{\partial R_f}{\partial z} \quad (2a)$$

where z is the vertical coordinate, t is time, and Δz is snow node thickness (m). $z = 0$ at the snow-soil interface (couple with the soil model through the fluxes) and $z = d_s$ at the snow surface (couple with the vegetation and atmospheric models through the fluxes). The boundary condition is:

$$R_f|_{z=d_s} = P_0 - E \quad (2b)$$

where P_0 is the effective rate of precipitation on land surface (downward) ($\text{kg m}^{-2} \text{ s}^{-1}$) (in BATS vegetation model (Dickinson *et al.*, 1993), precipitation in the vegetation portion will be intercepted by a 'vegetation-interception reservoir' and the excess drops on the land surface), and E denotes the rate of evaporation (upward) ($\text{kg m}^{-2} \text{ s}^{-1}$). Note: because of using the concept of 'liquid water-holding capacity', R_f needs no boundary condition at $z = 0$ (see below).

Energy conservation equation

The heat content (H) for a unit snow volume changes because of ice heat conduction and penetration of net solar radiation, R_s (in W m^{-2}):

$$\frac{\partial H}{\partial t} = \frac{\partial}{\partial z} \left(K \frac{\partial T}{\partial z} + R_s \right) \quad (3a)$$

where T is snow temperature (K), and K is snow thermal conductivity ($\text{W m}^{-1} \text{ K}^{-1}$). The boundary conditions (fluxes) at the surface and bottom of snow cover are expressed as:

$$\begin{aligned} \left(K \frac{\partial T}{\partial z} + R_s \right) \Big|_{z=d_s} &= R_s^n + L_{net} - I_{sen} - L_{lv} \cdot E + I_{prec}, \\ K \frac{\partial T}{\partial z} \Big|_{z=0} &= - \frac{2 \cdot K^1 \cdot K_{soil} \cdot (T^1 - T_{soil})}{K_{soil} \cdot \Delta z^1 + K^1 \Delta z_{soil}} \end{aligned} \quad (3b)$$

where R_s^n and L_{net} are net solar and long-wave radiation at snow surface (W m^{-2}); I_{sen} is sensible heat flux (W m^{-2}); L_{lv} denotes latent heat of evaporation (J kg^{-2}); I_{prec} is the heat flux of precipitation (W m^{-2}); K_{soil} is soil thermal conductivity ($\text{W m}^{-1} \text{ K}^{-1}$); K^1 is the thermal conductivity of bottom snow layer ($\text{W m}^{-1} \text{ K}^{-1}$); and T^1 and T_{soil} are temperatures from the bottom snow layer Δz^1 and the top soil layer Δz_{soil} , respectively.

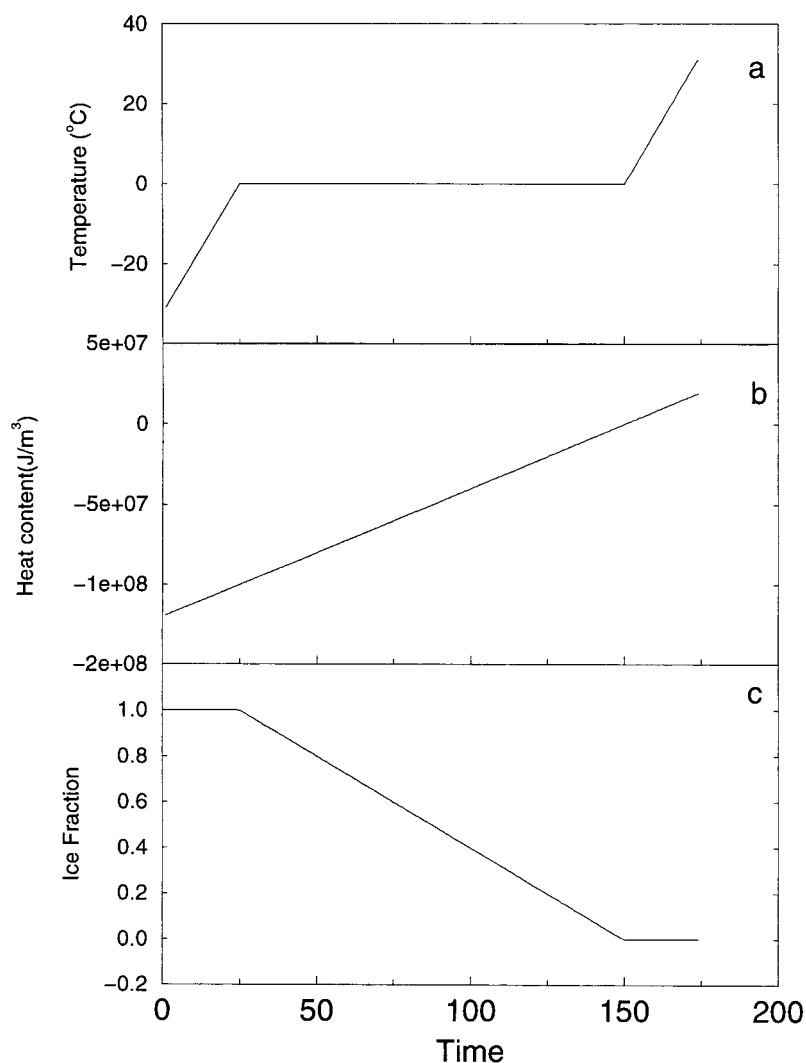


Figure 2. Determination among H , f_{ice} , and T in an ice-liquid water system

In equation (3a), the heat content (H in $\text{J m}^{-3} \text{K}$) is expressed as:

$$H = C_v \cdot (T - 273.15) - f_{ice} \rho_s L_{li} \quad (4)$$

where C_v is the volumetric specific heat of snow ($\text{J m}^{-3} \text{K}^{-1}$), and L_{li} is the heat of fusion (J kg^{-1}). Note that (a) H includes the internal energy of liquid water or ice as well as the energy of the phase change between liquid water and ice, and (b) the internal energy of liquid water at the melting point (273.15 K) is set at zero (a relative value). Figure 2 illustrates how the variables H , T , and f_{ice} of equation (4) change when a unit volume of pure ice is uniformly heated to pure liquid water. It can be seen that, if H has a zero or positive value, the system is in the pure liquid phase ($f_{ice} = 0$), with temperature at or above the melting point; if H has a negative value equal to or less than $-\rho_s L_{li}$, the system is in the pure ice phase ($f_{ice} = 1$) with temperature at or below the melting point, otherwise, the system is a mixture of liquid water and ice at the melting temperature, and the fractional variable (f_{ice}) is determined by the value of H . The continuous feature of H during phase change simplifies computation. In addition, by assuming liquid water energy equal to zero at the melting

Table II. Calculations for the right-hand terms in the governing equations and boundary equations

Thermal conductivity of snow (K) (Yen, 1965)	$K = 3.2217 \times 10^{-6} \cdot (\rho_s)^2 \quad (\text{w m}^{-1} \text{K}^{-1})$
Volumetric specific heat capacity of snow (C_v) (Verseghy, 1991)	$C_v = 1.9 \times 10^6 \frac{\rho_s}{\rho_i} \quad (\text{J K}^{-1} \text{m}^{-3})$
Solar radiation in a snowpack (R_s) (Jordan, 1991)	$R_s(z) = \begin{cases} R_s^n \cdot [e^{-0.002\beta_{nir}}(e^{-\beta_{vis}(d_s-z)} - 1) + 1] & \text{Top node} \\ R_s^n \cdot e^{-\beta_{vis}(d_s-z)-0.002\beta_{nir}} & \text{Interior nodes} \end{cases}$ Extinction coefficients: $\begin{cases} \beta_{nir} = 400.0 \\ \beta_{vis} = \frac{0.003795 \cdot \rho_s}{\sqrt{d}} \end{cases}$
Ice mass fraction of precipitation (f_{ice}) (Referenced in code of SNTHERM)	$f_{ice} = \begin{cases} 0.0 & T_{air} > 2.5^\circ\text{C} \\ 0.6 & 2.0^\circ\text{C} < T_{air} \leq 2.5^\circ\text{C} \\ 1 - [54.62 - 0.2(T_{air} + 273.15)] & 0.0^\circ\text{C} < T_{air} \leq 2.0^\circ\text{C} \\ 1.0 & T_{air} \leq 0.0^\circ\text{C} \end{cases}$
Partial density of ice in snowfall (γ_i) (LaChapelle, 1969)	$\gamma_i = \begin{cases} 0.0 & T_{air} > 2.5^\circ\text{C} \\ 189.0 & 2.0^\circ\text{C} < T_{air} \leq 2.5^\circ\text{C} \\ 50.0 + 1.7(T_{air} + 14.99)^{1.5} & -15^\circ\text{C} < T_{air} \leq 2.0^\circ\text{C} \\ 50.0 & T_{air} \leq -15^\circ\text{C} \end{cases}$
Heat flux of precipitation (I_{prec})	$I_{prec} = \begin{cases} C_l P_0 (T_p - 273.15) & \text{for rainfall} \\ C_v \frac{\Delta z_p}{\Delta t} (T_p - 273.15) - P_0 L_{li} & \text{for snowfall} \end{cases}$ where new snow thickness $\Delta z_p = \frac{P_0 \Delta t f_{ice}}{\gamma_i}$

point, the energy of the melt water flow becomes constant at zero and does not show in the energy equation (equation 3a); only the mass remains in the mass equation (equation 2a). The method was also used by Lynch-Stieglitz (1994) and Tarboton and Luce (1996).

In order to solve variables ρ_s , H , and Δz , we need to define the right-hand terms in the governing equations, i.e., liquid flow, ice heat conduction, and radiation penetration, as well as those in the boundary condition equations, i.e., the surface fluxes.

Anderson's (1976) formula for computing liquid water-holding capacity (C^R) from snow density is adopted in the model:

$$C^R = \begin{cases} C_{\min}^R & \gamma_i \geq \gamma_e \\ C_{\min}^R + (C_{\max}^R - C_{\min}^R) \frac{\gamma_e - \gamma_i}{\gamma_e} & \gamma_i < \gamma_e \end{cases} \quad (5)$$

where $C_{\min}^R = 0.03$, $C_{\max}^R = 0.1$, $\gamma_e = 200$ (kg m^{-3}), and $\gamma_i = \rho_s f_{ice}$ is partial density of ice (kg m^{-3}). The liquid water transport in the snow pack is not dynamically described. If the liquid water content in a snow layer exceeds the water-holding capacity, the excess amount drains to the underlying layer. Hence, flow of liquid water (R_f) is:

$$R_f = \begin{cases} 0 & f_{ice} \geq \frac{1}{1 + C^R} \\ [1 - f_{ice}(1 + C^R)] \frac{\rho_s \cdot \Delta z}{\Delta t} & f_{ice} < \frac{1}{1 + C^R} \end{cases} \quad (6)$$

Note that there is no constraint applied at the bottom of a snow pack ($z = 0$). Outflow from the snow pack will infiltrate into the soil through the soil model, and the excess water becomes the discharge (runoff).

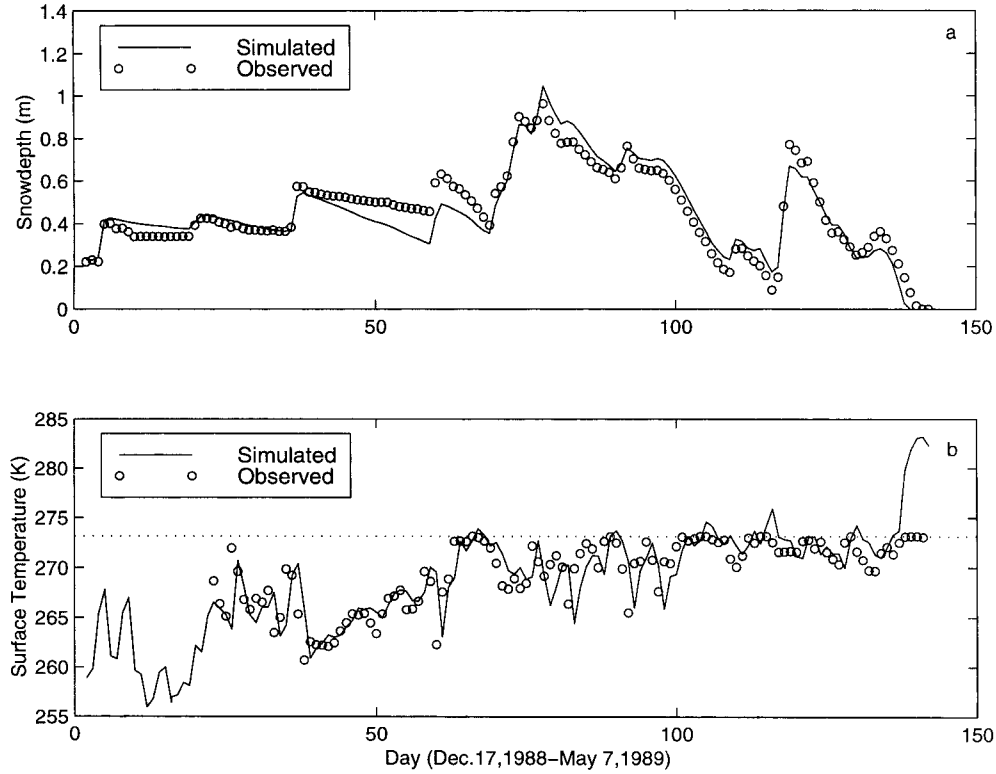


Figure 3. Comparisons of modelled snow depth and skin temperature with observations in the grassland at Col de Porte, France

Table III. Snow surface fluxes

(W/m ²)	Snow under the canopy	Snow on bare soil
Net surface solar radiation (R_s^n)		$I_s^{\downarrow} \cdot (1 - \alpha)$
Net long-wave radiation (L_{net})	$\epsilon_f \sigma T_f^4 - \sigma T_{sn}^4$	$\epsilon_{air} \sigma T_{air}^4 - \sigma T_{sn}^4$
Latent heat flux ($L_v E$)	$\rho_a W c f_g (q_{sn} - q_{af})$	$\rho_a W_G (q_{sn} - q_{air})$
Sensible heat flux (H_s)	$\rho_a c_p W_C (T_{sn} - T_{af})$	$\rho_a c_p W_G (T_{sn} - T_{air})$

The calculations relevant to the right-hand terms in the governing equations (i.e., thermal conductivity, solar radiation entering a snowpack) and those in the boundary equations (i.e., mass ice fraction of precipitation, partial density of ice in snowfall) are given in Table II. Table III shows the differences in calculating fluxes on snow surfaces under the canopy and in the open area. Note that the total flux is the area-weighted summation of fluxes from both portions. The calculations for snow albedo (Dickinson *et al.*, 1993) are given in the Appendix.

MODEL EVALUATION

French data set

The Centre d'Etude de la Neige in Grenoble, France measures both atmospheric forcing and snow properties at hourly intervals at the Col de Porte (45°N, 6°E, 1320 m a.s.l.) in the French Alps (Brun *et al.*, 1992). This site is characterized by a continuous snow cover in winter, usually lasting from late autumn to

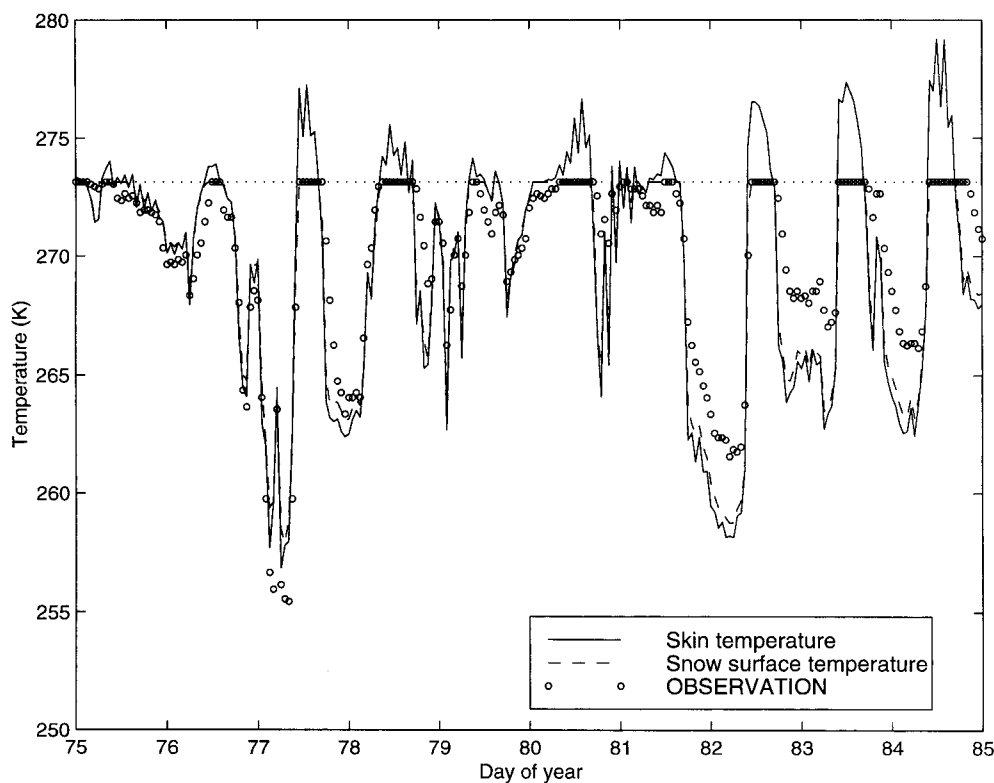


Figure 4. Comparisons of modelled snow surface temperature and skin temperature with the observations at Col de Porte, France

Table IV. Parameters of soil and vegetation (Dickinson, 1993)

	Col de Porte	BOREAS Southern Study Area
Vegetation type	Short grass (type 2)	Deciduous broadleaf tree (type 5)
Soil texture class	Type 4 (loam)	Type 6
Soil colour	Type 1	Type 3

late spring, with loamy soil and short-grass vegetation. Meteorological forcing data include air temperature, specific humidity, wind speed, precipitation amount, snow/rain index, downwelling solar, and long-wave radiation. Measured snow properties are snow depth, surface temperature, and daily albedo. The parameters for vegetation and soil types were selected from the BATS global soil/vegetation data base (Table IV). The simulation period was from 17 December 1988 to 7 May 1989.

Simulated snow depths agree well with observations (Figure 3a); however, simulated daily skin temperatures were slightly different from observed surface temperature (Figure 3b). On some days, simulated skin temperatures were above the melting point, while the observation temperatures remained at or below the melting point. This suggests that observed temperature was associated with a small snow-covered area, whereas skin temperature is the area-weighted mean of three different surface composites, i.e., snow, vegetation, and bare soil. Figure 4 shows that the diurnal skin temperature differed from the snow surface temperature, and the latter closely matched with the observations, especially during the day. Because of the low values of vegetation and bare soil albedo, the grid surface albedo was consistently lower than the observations, while the modelled snow surface albedo varied around the mean of the observed (Figure 5). Except for high-frequency variations in observed albedo, the simulation albedo as a function of surface snow

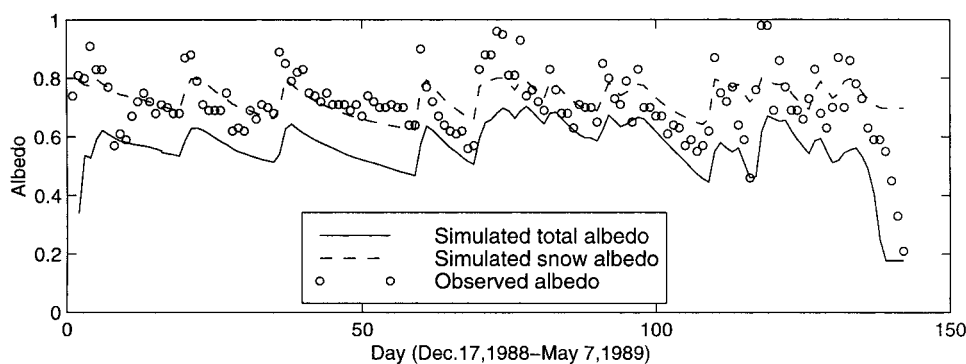


Figure 5. Comparisons of modelled snow surface albedo and surface albedo with the observations at Col de Porte, France

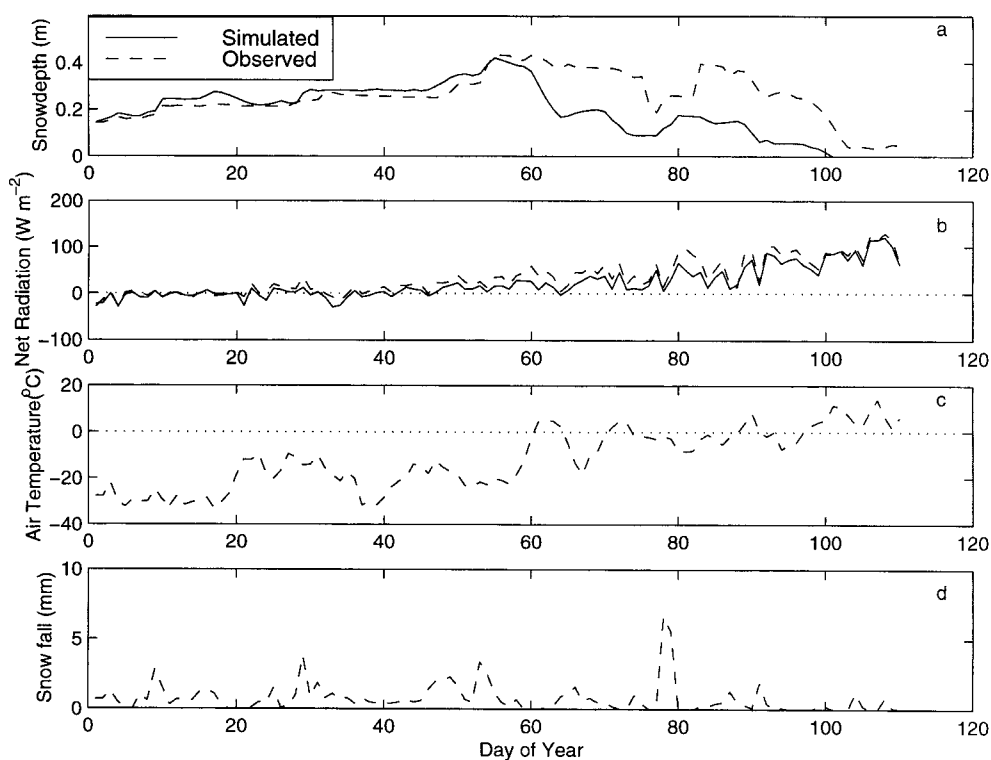


Figure 6. Comparisons of modelled (a) snow depth, (b) surface net radiation with the observations, (c) observed air temperature, and (d) observed snowfall snow in old aspen region of SSA at Boreal, Canada

age (Dickinson *et al.*, 1993) was quite satisfactory. Because observed albedo was not very reliable (Eric, pers. comm., 1998), further adjusting the model to match observed albedo was not warranted.

BOREAS data set

The second set of observations were collected at the southern intensive study areas of the Boreal Ecosystem Atmosphere Study (BOREAS), located on the southern edges of the Canadian boreal forest, 600 km from Prince Albert, Saskatchewan. BOREAS is a large-scale field investigation to study the interactions

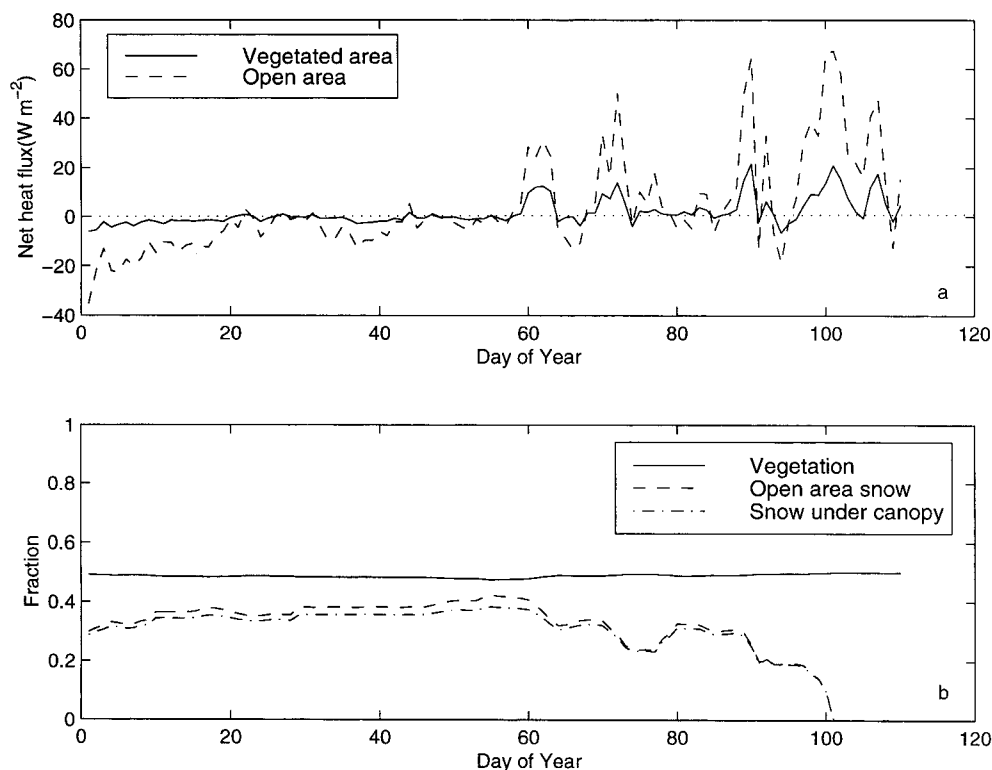


Figure 7. (a) Modelled net heat flux for the open area snow and under canopy snow, and (b) fractions of vegetation under canopy snow and open area snow in old aspen region of SSA at Boreal, Canada

between the boreal forest biome and the atmosphere, clarifying their roles in global change. The Southern Study Area (SSA) covers a domain large enough to allow the acquisition of useful airborne flux measurements and satellite observations, but small enough to conserve a reasonable density of surface instrumentation, including six towers of 20 m height for flux and meteorological measurements. In the BOREAS study areas, snow cover exists more than 100 days a year, and the forests of apes and pines provide strong interaction among the atmosphere, land surface, and snow cover. Because the BOREAS data are still under processing and only open to the project investigators, we were only able to use limited data in this very primary study. The 15-minute interval meteorological forcing and snow data at the old aspen site (53.628°N and 106.196°W) of the SSA were used in this study. The simulation period was 1 January (DOY 1) to 20 April (DOY 111), 1994. Model parameter values were taken from the BATS data base.

Before DOY 60, i.e., 2 March (the winter period), modelled and observed snow depth matched well while, after 2 March (the spring period), the model severely underestimated snow depth (Figure 6a), even though the modelled net radiation (a main energy source for snowmelt) in the spring period was still lower than the observed radiation (Figure 6b). In the spring season, net solar radiation was increased gradually, while the increase of air temperature involved four warm waves in which temperatures were above 0 °C for a few days (Figure 6c). Each of these warm waves corresponded to a marked reduction in modelled snow depth (Figure 6a), but not as severe in the observed snow depth. The snow protected by the canopy did not melt as quickly as in the open area and might still keep a thick snow depth which possibly was what observed. During the spring period, the modelled net surface energy for the open-area snow was several times stronger than that for the under-canopy snow (Figure 7a). Within the model, the sensible heat during these warm waves produced significant snowmelt in the open area, which consequently reduced the modelled (average)

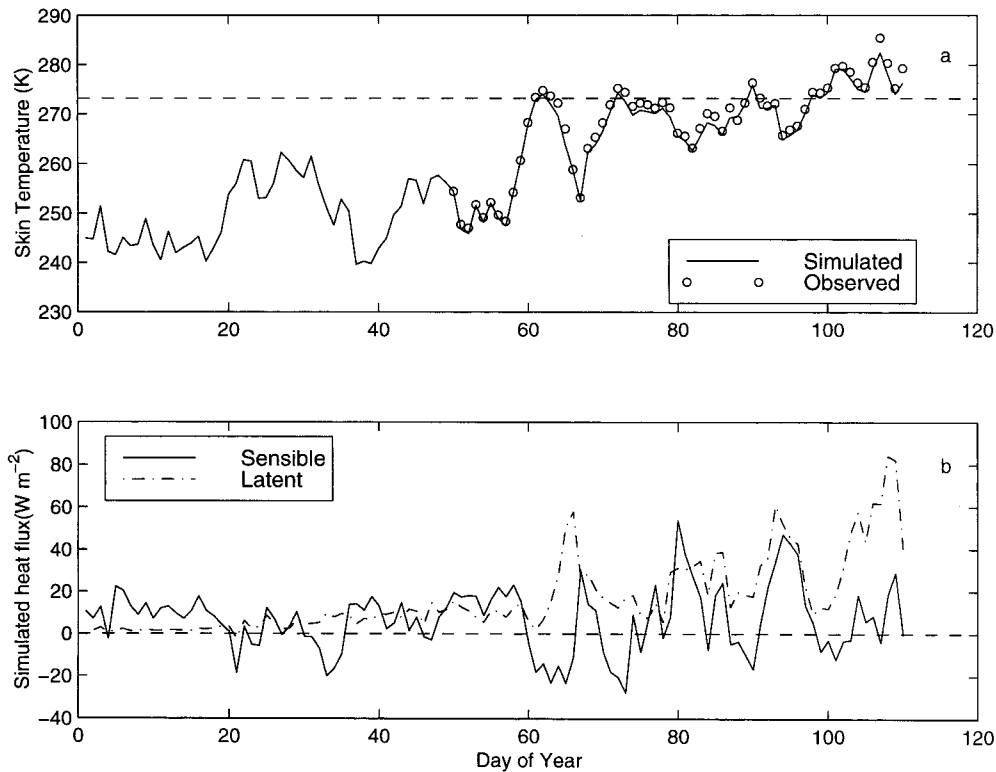


Figure 8. (a) Skin temperature and (b) surface energy fluxes in old aspen region of SSA at Boreal, Canada

snow depth. In Figure 7b, the fraction of snow under the canopy varied following that of the open-area snow, which indicated that the canopy snow could unrealistically ‘smear’ to the open area, because the model used ‘parameterization’ to simulate a single effective snow depth for the grid square. Differences between the observed and modelled snow depth in the spring period may be due in part to the area observed being only a subset of that modelled. In addition, uncertainties were found in the snow data. First, the snow depth data at the Prince Albert old jack pine site in the same area (Way *et al.*, 1997) showed a rapid decline in snow depth in the first warm period (DOY 60–63), which did not show in Figure 6a. Second, from Figure 6d, there seemed to be an insufficient amount of snowfall during DOY 81–83 to create an increase in snow depth shown in Figure 6a. Third, the snowfall and snow depth were not measured at the same places (Berry, pers. comm., 1998).

The simulated skin temperature matched with the observed surface temperature measured from the tower (Figure 8a). Figure 9 shows that the model simulated surface fluxes over vegetation, bare soil, and snow surface, separately, and also simulated a fraction of each. In the winter period, snow cover increased and the surface exchanges were depressed, while in the spring period, exchanges at the surface became important. Vegetation warmed and started to have upward sensible and latent heat fluxes. In contrast, the snow surface and bare soil became wetter than before but still colder than the air temperature; therefore, they had upward latent heat fluxes and downward sensible heat fluxes. The net result was a positive latent heat flux in spring and a highly variable sensible heat flux (Figure 8b). Unfortunately, because of equipment problems during cold weather, observations were not available. It is clear that, with such complex temporal variability and spatial heterogeneity over the forest landscape, a model with a separate simulation of different components is both necessary and useful.

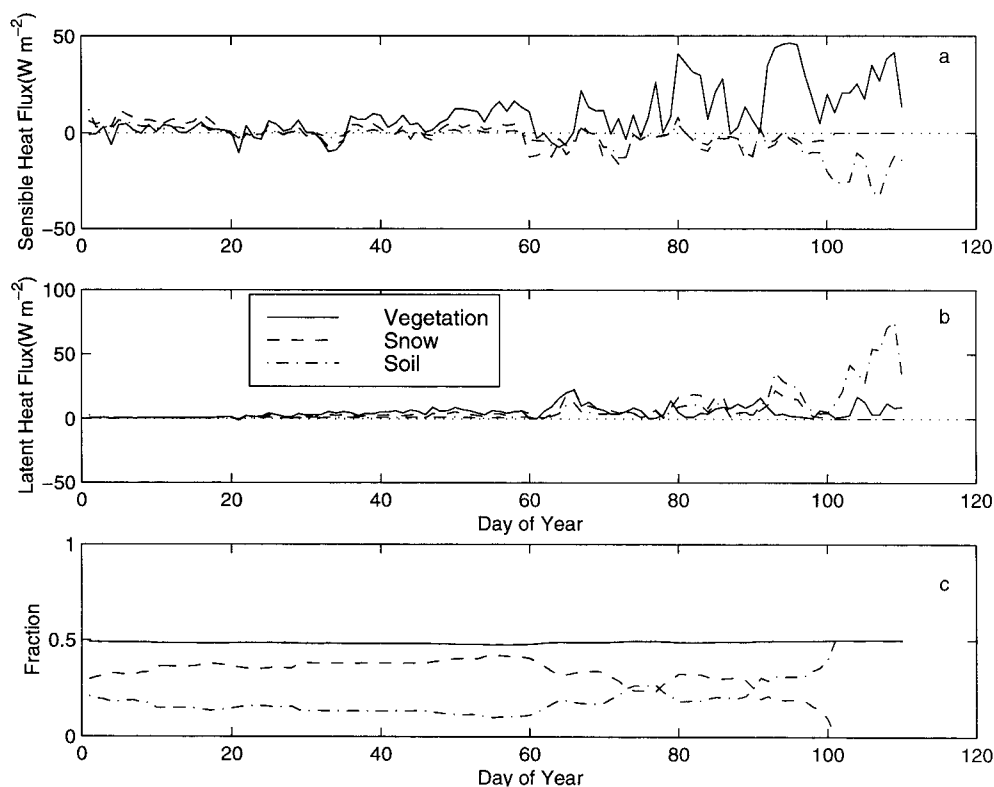


Figure 9. Deposition of surface energy fluxes into vegetation, snow, and bare soil contributions. (a) Sensible heat flux, (b) latent heat flux, and (c) fractional coverage of vegetation, snow, and bare soil

DISCUSSION

We realized that the setting of parameter values could substantially affect the simulation results. After comparing the soil and vegetation parameter values provided by the BOREAS documents (Coughlan and Running, 1994) with those used from the BATS data base, we found that they were close. Because most of the BOREAS document values were not measured in the field, we decided to use only the BATS parameter values.

The snow model presented here is not a point model, but represents the average features of an area characterized by the BATS data base. Because field observations are usually conducted at sites much smaller than the modelled area, they are expected to be different from the area means. Therefore, the comparison between the modelled results and field observations must be analyzed carefully to explore the suitability of the model, and the model should not be judged simply by agreement or disagreement. In this study, the model was driven by the observed meteorological forcing, and the model parameters were fixed without 'tuning'. We found that the simulations matched observations under two conditions: (a) when the study area was relatively uniform, such as in the short grass land, and (b) when the observations contained some kind of area-average features, such as the surface temperature and net radiation measured from a high tower. These provide the evidence that the model and its parameters are generally suitable for these study sites. The disagreements (besides caused by various errors) essentially resulted from the different scales between modeling and observation. Recently, in a BOREAS study, Hardy *et al.* (1997) showed that snow depth possessed substantial spatial variability, even around a single tree. Therefore, they used SNTHERM coupled

with a geometric optical-radiative transfer model (Li *et al.*, 1995) to conduct a series of point simulations along the observation locations.

CONCLUSIONS

The agreement of the modelled snow depth with the field observations using our three-layer snow model is consistent with the results from the multi-layer SNTHERM model at a range of seasonal and polar snow sites. Because of the substantial reduction of the computational requirement of our model compared to SNTHERM, our model is applicable for use in GCMs. It adds physical details of snow, such as melting and thawing, vertical and diurnal variability, to the current GCM snow submodels.

Introducing parameterization of subgrid heterogeneity into the snow model is a way of extending the point model to areas. The good agreement between modelled and observed skin temperature and albedo, and the reasonable explanation for the complicated responses of surface fluxes, indicate that this approach captured the essentials of subgrid heterogeneity, and its formulations and parameter values are representative.

ACKNOWLEDGEMENTS

Primary support for this research was provided under the NASA/EOS Interdisciplinary Research Program (NAG53640#1, NAG8-1520, and NAGW-2062) and the NOAA GCIP Program (NA46GP0247). The senior author, Jiming Jin, would like to thank the World Laboratory, International Centre for Scientific Culture (Switzerland) for selecting him as the first recipient of the John Harshbarger Fellowship. We thank Mete-France, Centre National de Recherche Meteorologiques, Centre D'etudes de la Neige for providing the Col de Porte data set. The careful reading and editing provided by Ms. Corrie Thies improved the manuscript.

REFERENCES

- Anderson EA. 1976. *A point energy and mass balance model of a snow cover*. Office of Hydrology, National Weather Service, Silver Spring, Maryland, NOAA Technical Report NWS 19.
- Berry JA. 1998. Personal communication.
- Bonan GB. 1996. A Land Surface Model (LSM version 1-0) for Ecological, Hydrological, and Atmospheric Studies: Technical Description and User's Guide. NCAR Technical Note, NCAR/TN-417 + STR, Boulder, Colorado, 150 pp.
- Brun E, David P, Sudul M, Brunot G. 1992. A numerical model to simulate snow cover stratigraphy for operational avalanche forecasting. *Journal of Glaciology* **38**(128): 13–22.
- Coughlan J, Running SW. 1994. First results of BOREAS modeling exercise #1 for workshop at Prince Albert, Saskatchewan, 23–25 July 1994. Appendix A, 13–18.
- Dickinson RE. 1988. The force-restore model for surface temperatures and its generalization. *Journal of Climate* **1**: 1086–1097.
- Dickinson RE, Henderson-Sellers A, Kennedy PJ. 1993. Biosphere Atmosphere Transfer Scheme (BATS) Version 1e as Coupled to the NCAR Community Climate Model. NCAR Technical Note, NCAR/TN-387 + STR, 72 pp.
- Douville H, Royer J-F, Mahfouf J-F. 1995. A new snow parameterization for the Mete-France climate model. Part I: validation in stand-alone experiments. *Climate Dynamics* **12**: 21–35.
- Eric M. 1998. Personal communication.
- Hardy JP, Davis RE, Jordan R, Li X, Woodcock C, Ni W, McKenzie JC. 1997. Snow ablation modeling at the stand scale in a boreal jack pine forest. *Journal of Geophysical Research* **102**: 29397–29405.
- Jin JM, Gao X, Yang Z-L, Bales RC, Sorooshian S, Dickinson RE, Sun SF, Wu GX. 1999. Comparative analyses of physically based snowmelt models for climate simulations. *Journal of Climate* **12**: 96–110.
- Jordan R. 1991. A one-dimensional temperature model for a snow cover. US Army Corps of Engineers, Cold Regions Research and Engineering Laboratory, Special Report 91-16, 49 pp.
- LaChapelle ER. 1969. Properties of Snow. Prepared for Hydrologic Systems course presented by College of Forest Resources, Nov. 17–18, University of Washington, Seattle, 21 pp.
- Li X, Strahler AH, Woodcock CR. 1995. A hybrid geometric optical-radiative transfer approach for modeling albedo and directional reflectance of discontinuous canopies. *IEEE Transaction Institute of Electrical and Electronics Engineers on Geoscience and Remote Sensing* **33**(2): 466–480.
- Loth B, Graf H-F, Oberhuber JM. 1993. Snow cover model for global climate simulations. *Journal of Geophysical Research* **98**: 10451–10464.
- Lynch-Stieglitz M. 1994. The development and validation of a simple snow model for GISS GCM. *Journal of Climate* **7**: 1842–1855.

- Marshall S, Roads JO, Glatzmaier G. 1994. Snow hydrology in a general circulation model. *Journal of Climate* **7**: 1251–1269.
- Pollard D, Thompson SL. 1995. Use of a land-surface-transfer scheme (LSX) in a global climate model: the response to doubling stomatal resistance. *Global and Planetary Change* **10**: 129–161.
- Tarboton DG, Luce CH. 1996. *Utah Energy Balance Snow Accumulation and Melt Model (UEB)*, Computer model technical description and user's guide. Utah Water Research Laboratory and USDA Forest Service Intermountain Research Station.
- Verseghy DL. 1991. CLASS-A Canadian land surface scheme for GCMs. Part I: soil model. *International Journal of Climatology* **11**: 111–133.
- Walland DJ, Simmonds I. 1996. Sub-grid-scale topography and the simulation of Northern Hemisphere snow cover. *International Journal of Climatology* **16**: 961–982.
- Way J, Zimmermann R, Rignot E, McDonald K, Oren R. 1997. Winter and spring thaw as observed with imaging radar at BOREAS. *Journal of Geophysical Research* **102**: D24, 29,673–29,648.
- Yang Z-L, Dickinson RE, Robock A, Vinnikov KY. 1997. Validation of the snow sub-model of the Biosphere-Atmosphere Transfer Scheme with Russian snow cover and meteorological observational data. *Journal of Climate* **10**: 353–373.
- Yen YC. 1965. Heat transfer characteristics of naturally compacted snow. US Army Cold Regions Research and Engineering Laboratory, Research Report 166, Hanover, NH, 9 pp.

APPENDIX

Snow surface albedo

$$\begin{aligned}\alpha &= 0.5(\alpha_{VIS} + \alpha_{IR}), \\ \alpha_{VIS} &= 0.95 \cdot (1 - 0.2f_{age}) + 0.4 \cdot f_Z \cdot [1 - 0.95 \cdot (1 - 0.2f_{age})], \\ \alpha_{IR} &= 0.65 \cdot (1 - 0.5f_{age}) + 0.4 \cdot f_Z \cdot [1 - 0.65 \cdot (1 - 0.5f_{age})],\end{aligned}$$

Factor of snow age:

$$\begin{aligned}f_{age} &= \tau_s / (1 + \tau_s), \\ \tau_s^{N+1} &= (\tau_s^N + \Delta\tau_s)[1 - \max(0, P_o\gamma_i\Delta t)/10], \\ \Delta\tau_s &= (r_1 + r_2 + r_3)\Delta t / \tau_0,\end{aligned}$$

$$\tau_0 = 1 \times 10^6 \text{ s}; \quad r_1 = \exp\left[5000\left(\frac{1}{273.16} - \frac{1}{T_s}\right)\right]; \quad r_2 = (r_1)^{10} \leq 1; \quad r_3 = \begin{cases} 0.01 & \text{Antarctica} \\ 0.30 & \text{elsewhere} \end{cases}$$

Factor of solar zenith angle:

$$f_Z = \frac{1}{2} \left[\frac{3}{1 + 4 \cos \theta_Z} - 1 \right], \quad \text{when } \cos \theta_Z \geq 0.5, f_Z = 0 \text{ and } \cos \theta_Z = 0, f_Z = 1.$$